The Importance of the Helix 2 Region for the *cis*-Cleaving and *trans*-Cleaving Activities of Hepatitis Delta Virus Ribozymes†

Chuan-Bin Lee,‡ Yen-Chein Lai,‡,§ Yueh-Hsin Ping,‡ Zhi-Shun Huang,‡ Jung-Yaw Lin,§ and Huey-Nan Wu*,‡

Institute of Molecular Biology, Academia Sinica, Taipei, Taiwan, and Institute of Biochemistry, College of Medicine, National Taiwan University, Taipei, Taiwan

Received May 21, 1996; Revised Manuscript Received July 16, 1996⊗

ABSTRACT: The sequence, secondary structure, and size requirements of the helix 2 region (H2) of a *cis*-acting hepatitis delta virus ribozyme Rz 1 were examined in this study. Mutational analysis was performed, and the cleavage rate of each H2 mutant of Rz 1 was assayed. We found that H2 could be elongated to twice its original size without affecting ribozyme folding while the shortening of H2 by one base pair severely decreased autolytic activity. In addition, the maintenance of the Watson−Crick base-pairing interactions of the last base pair of H2 (A16U58) was not critical for *cis*-cleavage reaction. Nevertheless, mutants with an AA, an AG, an AC, or a GG pair at the bottom of H2 were less active, and the sequence of the H2/H3 interface might affect the stability of the catalytic core. The negative effects on ribozyme folding, such as the destabilization of H2, the unfavorable sequences at the last base pair of H2 as well as the disruption of the continuity of H2 and H3, could be compensated for by elongating the H2 region of the corresponding mutants. The extension of H2 may alter the conformation of ribozyme molecules; in addition, it stabilized the catalytic core and enhanced the resistance to formamide. Finally, for a *trans*-acting ribozyme and its substrate that require the formation of H1, H2, and H4 to reconstitute the autocatalytic domain of HDV RNA, the extension of H2 stabilized the substrate/ribozyme complex and speeded up the cleavage rate but hindered the product release process.

Hepatitis delta virus (HDV)[1] contains a single-stranded circular RNA of 1.7 kb as genome (Kos et al., 1986; Wang et al., 1986; Makino et al., 1987). The HDV RNA of genomic and antigenomic senses *cis*-cleave *in vitro* (Kuo et al., 1988). This site-specific cleavage reaction is an essential process for the replication of HDV RNA (Macnaughton et al., 1993). The autocatalytic activity requires the presence of magnesium ion or other divalent cations, and the reaction products contain a 5′-hydroxyl group and a 2′,3′-cyclic phosphate group (Wu et al., 1989; Suh et al., 1993). Extensive mutational analysis has been carried out to define the boundaries, identify the sequence requirement, and investigate the secondary structure of the autolytic domain of each sense of HDV RNA (Kuo et al., 1988; Rosenstein & Been, 1991; Wu et al., 1992; Wu & Huang, 1992). Two domains have many common features that are different from other well-characterized catalytic RNA's such as the hammerhead and hairpin ribozymes (Uhlenbeck, 1987; Hampel et al., 1990). The HDV autolytic domain contains four base-pairing regions and each helical region has its characteristics: H1 and H3 are restricted in size, the sequence of H2 is not critical, and the long self-complementary region (H4/Lp4) can be replaced by a stable hairpin loop (Wu et al., 1992, 1993; Wu & Huang, 1992). These double-stranded regions may fold into a pseudoknot-like structure (Perrotta & Been, 1991). Moreover, the residues enclosed by H3, the residues connecting H1 and H4, and the residues between H4 and H2 have stringent sequence requirements (Kummar et al., 1992; Kawakami et al., 1993; Thill et al., 1993; Tanner et al., 1994). These residues may be involved in the formation of the catalytic core; in addition, some of them may directly participate in catalysis.

Several variants of the HDV autolytic domains that *cis*-cleaved efficiently have been constructed on the basis of the findings of mutational analysis (Wu & Huang, 1992; Wu et al., 1993). These HDV ribozymes may retain the essential structure and sequence elements of the native HDV autolytic domains. Furthermore, the *cis*-acting HDV ribozymes have been converted into various bimolecular constructs, and the ribozyme subdomains catalyze the site-specific cleavage of the corresponding substrate subdomains *in trans* (Lai et al., 1996). Therefore, the proposed pseudoknot-like structure of the HDV autolytic domain could be reconstituted after two subdomains were associated through base-pairing interactions.

The H2 of the HDV autolytic domain is proposed to form a coaxial helix with H3 in the pseudoknot-like structure model. In this report, we studied the effect of the shortening, the elongation, and the disruption of the helical structure of H2 on the autolytic activity of a *cis*-acting HDV ribozyme. Moreover, whether the sequence of the last base pair of H2 that was at the interface of H2 and H3 affected *cis*-cleavage reaction and the importance of the maintenance of the coaxial stacking helices were investigated as well. Furthermore, the effect of H2 extension on the formation of substrate/ribozyme complex and the cleavage rate and cleavage product release

†This work was supported by Academia Sinica and a grant from National Science Council, ROC (NSC-84-2331-B-001-007 MH).

* Corresponding author. FAX: +886-2-782-6085. E-mail: hnwu@gate.sinica.edu.tw.

‡ Academica Sinica.

§ National Taiwan University.

⊗ Abstract published in *Advance ACS Abstracts*, September 1, 1996.

[1] Abbreviations: H1, H2, H3, and H4, helix 1, helix 2, helix 3, and helix 4; HDV, hepatitis delta virus; PCR, polymerase chain reaction; EDTA, ethylenediaminetetraacetic acid; $t_{1/2}$, half-life; CIP, calf intestine phosphotase; DTT, dithiothreitol; S, substrate; R, *trans*-acting ribozyme.

S0006-2960(96)01219-6 CCC: $12.00

process of a site-specific cleavage reaction catalyzed by a *trans*-acting HDV ribozyme were examined. The results illustrated that H2 is an essential structural element of HDV autolytic domain. The elongation of H2 may stabilize the catalytic core and enhance the cleavage rate of both *cis*- and *trans*-acting HDV ribozymes.

MATERIALS AND METHODS

Constructs, Templates for RNA Synthesis, and Preparation of RNA's. Rz 1 is a *cis*-cleaving HDV ribozyme (Lai et al., 1996). In construct Rz 1, the cDNA of ribozyme sequence was placed downstream of a T7 promoter and between a *Kpn*I site and a *Hin*dIII site. Different mutants of Rz 1 were created by PCR (polymerase chain reaction) mediated mutagenesis with appropriate synthetic DNA as primers. The PCR product that contained a T7 promoter followed by the cDNA of ribozyme mutant was cloned to pUC19. The sequence of each construct was confirmed by DNA sequencing (Sanger et al., 1977). Rz 1 and its mutants were *Hin*dIII run-off transcripts. The templates for the synthesis of the *trans*-acting ribozymes (RNA37 and LH2RNA37) and their corresponding substrate (RNA73) were PCR products. The PCR products were directly used as templates for RNA synthesis without further purification. The internally ^{32}P-labeled RNA's for *cis*- and *trans*-cleavage reactions were synthesized by T7 RNA polymerase *in vitro* transcription reactions. The synthesis, purification and quantitation of RNA fragments followed the procedures described by Lai et al. (1996).

Cleavage Reactions. The pretreatment of RNA molecules, the conditions to conduct *cis*-cleavage reaction, and the determination of the extent of cleavage, i.e., the fraction of the reactive RNA species at the end of reaction, followed those of Lai et al. (1996). For the *cis*-cleavage reactions conducted in the presence of formamide, the RNA molecules were denatured in the presence of various concentrations of formamide at 95 °C for 1.5 min. The RNA solution was then cooled down to room temperature and incubated at 50 °C for 5 min before the initiation of cleavage by 40 mM Tris-HCl, pH 7.5, and 12 mM $MgCl_2$.

For most of the *trans*-cleavage reactions of this study, the substrate and ribozyme RNA's were denatured and renatured together to promote annealing. The *trans*-cleavage was then initiated by adding a solution containing Tris-HCl (pH 7.5) and $MgCl_2$ with the final concentrations of 40 mM and 12 mM, respectively. The reaction was performed at 50 °C. Alternatively, the substrate RNA and ribozyme RNA were denatured and renatured separately, preincubated with Tris-HCl/$MgCl_2$ solution for 5 min. And two RNA solutions were then mixed to initiate *trans*-cleavage (Lai et al., 1996).

The cleavage reaction was terminated by the stop solution containing 50 mM of EDTA and 7 M of urea. The rate constants for the first order disappearance of the reactive precursor RNA in *cis*-cleavage reactions (k) and the reactive substrate RNA in single-turnover *trans*-cleavage reactions (k_{ob}) were determined (Lai et al., 1996). The $t_{1/2}$ of *cis*-cleavage reaction was obtained by dividing 0.693 with the rate constants (k).

Structural Probing. Transcription reactions were performed to obtain the precursor RNA of variant A16G58 and the 3′ cleavage products of Rz 1, variants A16G58.H2 and Rz 1.H2. The RNA was located by UV shadowing after electrophoresis. Then the absorbency at 260 nm was detected and the concentration of each purified RNA fragment was calculated by assuming the extinction coefficient to be 6.6×10^3 M^{-1} cm^{-1} per residue. The 5′-triphosphate group of the precursor RNA was removed by calf intestine phosphotase (CIP). T4 polynucleotide kinase was used for 5′-end labeling, and a 10 μL reaction contained ~2 pmol of RNA, 2 pmol of [γ-^{32}P]ATP (6000 Ci/mmol), 70 mM Tris-HCl (pH 7.6), 10 mM $MgCl_2$, 5 mM DTT, and 5 units of enzyme. After 1 h of incubation at 37 °C, the reaction was terminated by EDTA and urea. The end-labeled RNA was gel purified.

The 5′-end labeled RNA (20 000−30 000 cpm for nuclease digestion and 100 000 cpm for alkaline hydrolysis) that had been denatured at 95 °C for 3 min and cooled down to room temperature beforehand was incubated with 50 μg of carrier tRNA in appropriate reaction buffer at 37 °C for 10 min. The nuclease digestion reaction was initiated by the addition of 1 or 2 μL of 2×10^{-2} units/μL of RNase T1 or 7×10^{-3} units/μL of RNase V1 with the final volume of 10 μL. The RNase T1 digestion reaction was performed in 40 mM Tris-HCl (pH 8.0), 1 mM EDTA, and 10 mM $MgCl_2$ at 37 °C for 10 min. The RNase V1 digestion reaction was conducted in 25 mM Tris-HCl (pH 8.0), 200 mM NaCl, and 10 mM $MgCl_2$ at 37 °C for 10 or 20 min. The alkaline hydrolysis ladders were generated by heating the RNA in 50 mM $NaHCO_3$/Na_2CO_3 (pH 9.6) at 100 °C for 3 min. To terminate the digestion and hydrolysis reactions, an equal volume of 95% formamide/0.02% bromophenol blue/0.02% xylene cyanol was added and the mixture was frozen in a dry ice/ethanol bath. Samples were heated at 95 °C for 1.5 min before being analyzed by a 10% polyacrylamide gel containing 7 M urea.

RESULTS AND DISCUSSION

The cis-Cleaving Ribozyme

Rz 1 (Figure 1A) was derived from the autolytic domain of HDV RNA by internal substitution and deletion. There are four helices, i.e., H1, H2, H3, and H4, in Rz 1 that may fold into a pseudoknot-like structure. Rz 1 *cis*-cleaved efficiently, and the rate of the first-order reaction was 0.46 min^{-1} ($t_{1/2}$ = 1.5 min) in the presence of 12 mM of magnesium ion at 50 °C (Table 1). Mutational analysis was conducted in this study to investigate the role of H2 on the *cis*-cleavage reaction of HDV ribozyme. Since a correctly folded RNA is required for autolytic reaction and the rate of cleavage is likely to be limited by the rate of folding, the effect of H2 mutation on ribozyme folding can then be evaluated.

H2 Deletion, Substitution, and Insertion Mutants. Variants H2-1, H2-2, and H2-3 that had three or five AU base pairs inserted to different locations of H2 cleaved at rates comparable to that of Rz 1 (Figure 1D). In addition, the insertion of 5′-C_2A_2-3′ to A62/A63 of Rz 1 that may elongate H2 at the expense of shortening $J_{1/2}$ elevated the cleavage rate by ~3-fold (variant Rz 1.H2, Figure 1B and Table 1). The high autolytic activity of these insertion mutants disclose that the elongation of H2 does not affect the catalytic core of HDV ribozyme and H2 is not likely to have stringent sequence requirement. Therefore, H2 may protrude away from the catalytic core.

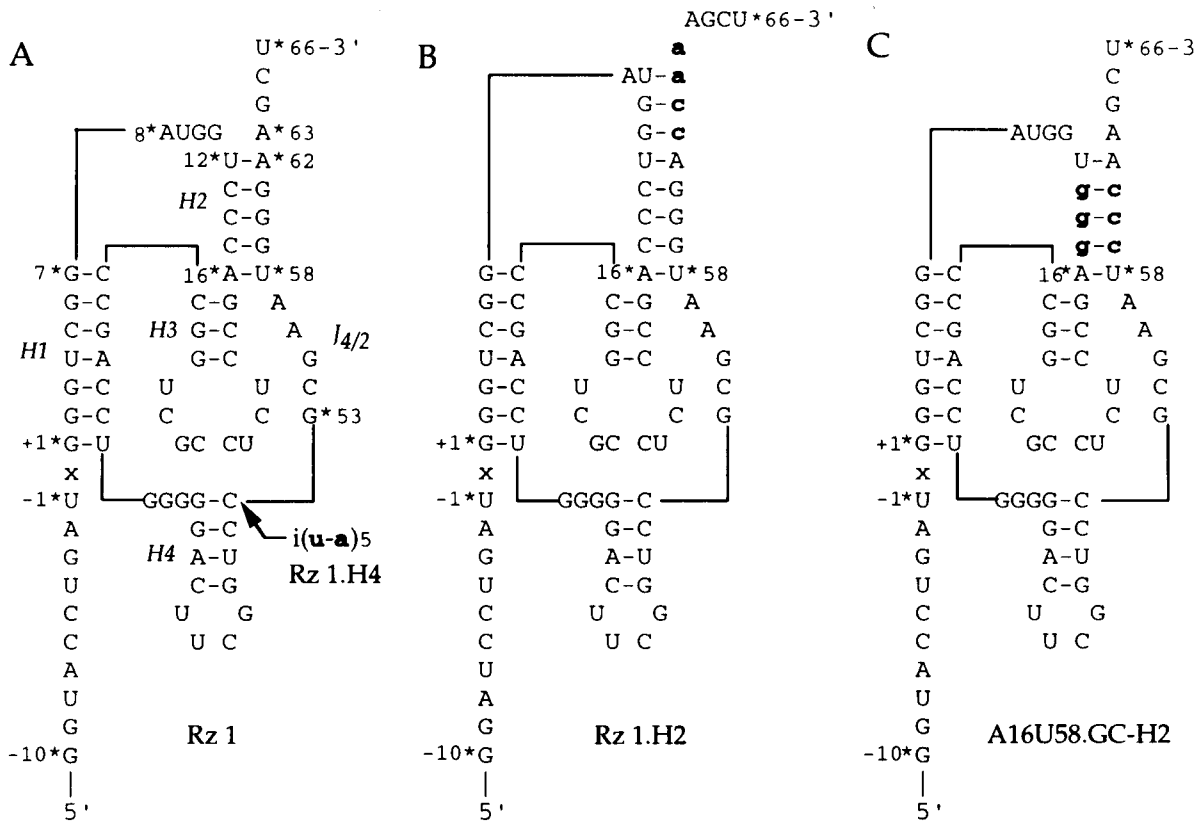

D

Rz 1 (wt)	Δ16Δ58	G61A	H2-1	H2-2	H2-3
[1.5'; (90%)]	[(20%) 6hr]	[(20%) 4hr]	[1'; (90%)]	[1'; (90%)]	[2'; (50%)]

H2-4	H2-5	H2-6	H2-7	H2-8
[10'; (60%)]	[6'; (70%)]	[5'; (50%)]	[10'; (70%)]	[10'; (80%)]

FIGURE 1: A, B, and C are the sequences and proposed secondary structures of Rz 1, Rz 1.H2, and A16U58.GC-H2, respectively. The Rz 1.H4 in (A) is an insertion mutant of Rz 1 that has five UA base pairs inserted to the top of the H4 of Rz 1. H1, H2, H3, and H4 are the four double-stranded regions; $J_{4/2}$ is the single-stranded region connecting H4 and H2; "x" is the cleaving point. (D) The helix 2 (H2) mutants of Rz 1. Only the sequence of the H2 region of each mutant is shown. The substituted or inserted residues are illustrated by lower case bold letters and "Δ" indicates that the residue has been deleted. The *cis*-cleavage reaction was conducted in the presence of 40 mM Tris-HCl (pH 7.5) and 12 mM $MgCl_2$ at 50 °C after the RNA was denatured and renatured. The $t_{1/2}$ of the *cis*-cleavage reaction of reactive RNA species and the molar ratio of the reactive RNA molecules of each variant are shown.

In contrast, variant Δ16Δ58 that had both A16 and U58 deleted and variant G61A that had one base pair mismatched near the top of H2 *cis*-cleaved poorly in the presence of 12 mM $MgCl_2$ (Figure 1D). Thus, the shortening as well as

Table 1: Summary of the Half-Lives of the *cis*-Cleavage Reactions of Ribozyme Rz 1 and Its Mutants

variant[a]	$t_{1/2}$ (50 °C)[b]	H2 extended variant[a]	$t_{1/2}$ (50 °C)[b]
Rz 1 (wt, A16U58)	1.5′	Rz 1.H2 (A16U58.H2)	0.5′
Mutants with a Bulged Residue at the H2-H3 Interface			
A16Δ58	CS[c]	A16Δ58.H2	60′
G16Δ58	CS[c]	G16Δ58.H2	45′
Substitution Mutants of Positions 16 and 58			
G16U58	1′		
U16U58	1′		
C16U58	2′		
A16G58	50′	A16G58.H2	5′
A16C58	70′	A16C58.H2	10′
A16A58	50′		
C16G58	1′	C16G58.H2	1.5′
G16C58	1′	G16C58.H2	2′
U16A58	1′		
U16G58	10′	U16G58.H2	8′
U16C58	3′	U16C58.H2	10′
C16C58	6′	C16C58.H2	1′
C16A58	10′	C16A58.H2	2′
G16A58	2′	G16A58.H2	8′
G16G58	65′	G16G58.H2	2′
Mutants with the CG Pairs of H2 Flip-Flopped			
A16U58.GC-H2	1′		
A16G58.GC-H2	30′		
A16C58.GC-H2	45′		
A16A58.GC-H2	8′		

[a] Variants N16N58 and N16Δ58 were derived from Rz 1, variants N16N58.H2 and N16Δ58.H2 were derived from Rz 1.H2, and variant A16N58.GC-H2 was derived from A16U58.GC-H2 by substituting or deleting the residue(s) of the last base pair of H2. [b] The *cis*-cleavage reaction was conducted in 40 mM Tris-HCl (pH 7.5) and 12 mM $MgCl_2$ at 50 °C. The "$t_{1/2}$" is the half-life of the first-order *cis*-cleavage reaction of the reactive RNA species. [c] CS represents only 20% of the RNA molecules *cis*-cleaved after 6 h of incubation.

the disruption of H2 severely decreased autolytic activity. Nevertheless, mutants of variant H2-3 that had one or two base pairs of the eight base-pair H2 mismatched *cis*-cleaved at rates only 2−5-fold slower than that of H2-3 (variants H2-4 to H2-8, Figure 1D). Each of these five mutants was more reactive than that of variant G61A. The results reveal that the extension of H2 may counteract the negative effect of the disruption of the base-pairing interaction in H2 on ribozyme folding.

Importance of Coaxially Stacked Helixes. The importance of the costacking of H2 and H3 for the folding of HDV *cis*-cleaving ribozyme was examined by introducing a bulged residue to the helix−helix interface. Two mutants were constructed. Each of them had the U58 of variant Rz 1.H2 deleted and had an A or a G at position 16. Both mutants (A16Δ58.H2 and G16Δ58.H2) cleaved at a rate ∼100-fold slower than that of Rz 1.H2 (Table 1). Thus, the interruption of the stacking of H2 and H3 may severely affect the folding of ribozyme molecule. Nevertheless, the bulged residue at the interface of H2 and H3 had a more profound effect on ribozymes containing a shorter H2. Variants A16Δ58 and G16Δ58 of Rz 1 were much less active than variants A16Δ58.H2 and G16Δ58.H2 (Table 1). The result also reveals that the extension of H2 has positive effect on ribozyme folding.

A16U58 Substitution Mutants of Rz 1. The H2 and H3 of HDV ribozyme have been proposed to stack coaxially in the pseudoknot-like structure model. The thermodynamic studies of a model system illustrate that the stability of coaxial stacking interaction depends on the sequences of helix−helix interfaces (Walter & Turner, 1994). We then examined whether the sequence of nucleotides 16 and 58 of Rz 1 that locate at the interface of the proposed coaxial helixes affects the folding of HDV ribozyme. The A16U58 of Rz 1 were replaced with all possible sequences. The rate of *cis*-cleavage of each mutant was assayed, and the results were summarized in Table 1.

The mismatch of the last base pair of H2 (A16U58) by substituting A16 to other sequences had almost no effect on *cis*-cleavage reaction since variants G16U58, U16U58, and C16U58 were as active as Rz 1. The replacement of the U58 by a G, a C, or an A, in contrast, decreased the rate of *cis*-cleavage 30−50-fold (variants A16G58, A16C58, and A16A58, respectively). Nevertheless, the autolytic activities of these position 58 substitution mutants could be restored by the compensatory mutations at position 16 since variants C16G58, G16C58 and U16A58 *cis*-cleaved at rates comparable to that of Rz 1. The positions 16 and 58 substitution mutants U16G58, U16C58, C16C58, C16A58, and G16A58 *cis*-cleaved at rates only 2−6-fold slower than that of Rz 1, whereas, the substitutions in variant G16G58 decreased the rate of *cis*-cleavage ∼40-fold. Therefore, although all of the least active mutants had the last base pair of H2 mismatched, not all of the positions 16 and 58 mismatched mutants possessed lower autolytic activity. The maintenance of the base-pairing interaction of the last base pair of H2 may be important but is not critical for the folding of HDV ribozyme. Similar conclusion has been obtained from the mutational analysis of the homologous base pair of another HDV ribozyme (Tanner et al., 1994). Nevertheless, since the assay conditions were different, it is hard to directly compare the relative autolytic activity of individual mutants.

Moreover, the insertions of 5′-C_2A_2-3′ to the A62/A63's of variants A16G58, A16C58, and G16G58 significantly elevated their cleavage rates (variants A16G58.H2, A16C58.H2, and G16G58.H2, respectively, Table 1). Nevertheless, the same insertion had relatively small effects on the rate and the extent of cleavage of other A16U58 substitution mutants. The variants were listed in Table 1. Thus, the elongation of H2 may compensate for the negative effect of unfavorable sequences at the helix−helix interface as well.

Two of the least active A16U58 substitution mutants of Rz 1 contain a G at position 58. It is possible that the U12-C15 of variants A16G58 and G16G58 form base pairs with G58-G61 instead of G59-A62. The formation of the alternative H2 that introduces a bulge residue in the coaxial helixes rather than the mismatch of the last base pair of H2 may account for the low autolytic activities of these two mutants. To investigate this, we flip-flopped the CG pairs of Rz 1, i.e., C13-C15/G61-G59, and re-examined the effect of U58 to G58 substitution on *cis*-cleavage reaction. The replacement of three CG pairs with three GC pairs alone had no detectable effect (variant A16U58.GC-H2, Figure 1C and Table 1). Nevertheless, the co-substitution of the last base pair of H2 to A16G58 decreased cleavage rate ∼30-fold (variant A16G58.GC-H2, Figure 1C and Table 1). This finding rules out the possibility that the formation of the alternative H2 is the main cause of the lower autolytic activity of variant A16G58. Furthermore, the replacement of the A16U58 of variant A16U58.GC-H2 with an AA pair and an AC pair decreased the rate of *cis*-cleavage 8- and 45-

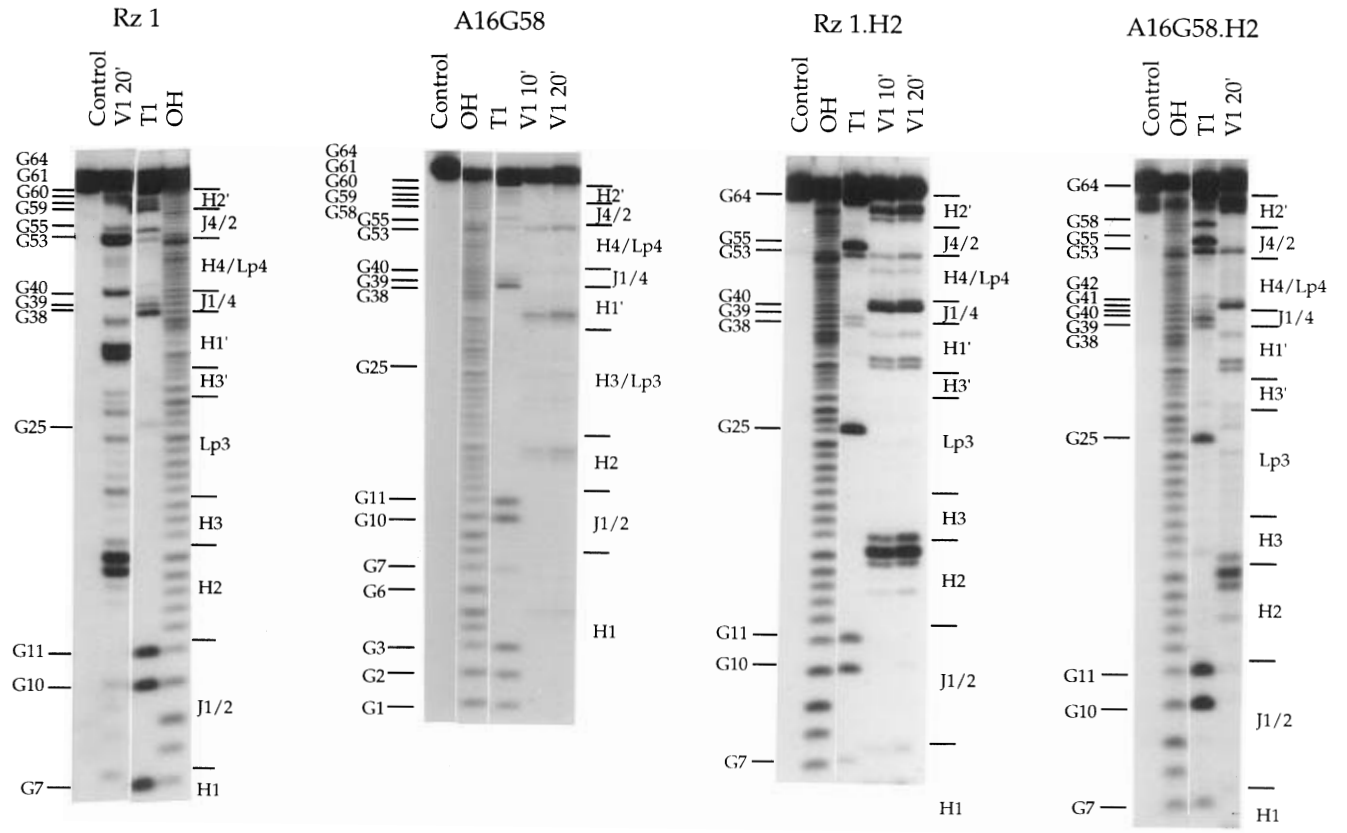

FIGURE 2: Probing the structures of different variants. The structures of the full-length RNA of variant A16G58 as well as the 3′ cleavage products of Rz 1, variant Rz 1.H2, and variant A16G58.H2 were probed by RNases. "Control" represents the RNA without any treatment; "OH" is the alkaline hydrolysis reaction; "T1" is the RNase T1 digestion reaction; and "V1 10′" and "V1 20′" indicate that the RNA was treated by RNase V1 for 10 and 20 min, respectively. H1, H1′, H2, H2′, H3, H3′, Lp3, H4-Lp4, $J_{1/2}$, $J_{1/4}$, and $J_{4/2}$ represent different sequence domains of ribozyme molecule.

fold, respectively (variants A16A58.GC-H2 and A16C58.GC-H2, Table 1). Therefore, similar to that of Rz 1, AA, AC, and AG are the less favorable sequences of the last base pair of H2 of variant A16U58.GC-H2 as well. The results confirm that the sequence of the H2−H3 interface may affect the autolytic activity of HDV ribozyme.

Effect of H2 Elongation on Folding of the Ribozyme Molecule. To detect the effect of H2 elongation on ribozyme folding, we probed the secondary structures of Rz 1 and variants A16G58, Rz 1.H2, and A16G58.H2 with RNases T1 and V1 in the presence of 10 mM of magnesium ion. The structures of the 3′ cleavage products rather than the precursor RNA's of the former three ribozymes were studied. We think this was justified since the catalytic domain of HDV ribozyme appears to reside entirely in the sequence 3′ to the cleavage site (Perrotta & Been, 1990, 1991). This speculation is supported by the finding that the RNases T1 and V1 digestion pattern of the 3′ cleavage product of variant A16G58 was almost indistinguishable from those of the uncleaved precursor RNA (data not shown).

Regardless of the mismatch by the U58 to G58 substitution at the last base pair of H2, the digestion patterns of variants A16G58.H2 and Rz 1.H2 were almost indistinguishable. In addition, Rz 1 and variant A16G58 also shared similar digestion patterns (Figure 2). However, it is notable that the elongation of H2 altered the RNase digestion patterns. The 3′ strand of H2 of variants Rz 1.H2 and A16G58.H2 were readily accessible to nuclease V1. Consistently, the G59, G60, and G61 of these two variants were resistant to RNase T1, whereas the residues of the same region of Rz 1 and variant A16G58 were either weakly digested (the former) or barely accessible to nuclease V1 (the latter). The results illustrate that the elongation of the complementary sequences between two strands of H2 enhances the stacking interactions among the residues of the 3′ strand of H2 and stabilizes the helical structure of H2. However, since the G10 and G11 of both variants Rz 1.H2 and A16G58.H2 were susceptible to RNase T1, the base-pairing interactions between the inserted 5′-C_2A_2-3′ and the residues of the $J_{1/2}$ region may not be stable enough to maintain the helical structure because of steric constrains. Alternatively, the stong RNase T1 cuttings in the $J_{1/2}$ region of these H2 extended mutants may be due to secondary digestion. Some other features were associated with the variants containing an extended H2: the G25 of Lp3 as well as the G53 and G55 of $J_{4/2}$ became readily accessible to RNase T1 while the G residues of $J_{1/4}$ became less susceptible to RNase T1; in addition, the 3′ strand of H1 was less sensitive to RNase V1, and the stronger RNase V1 cutting sites were switched from the 3′ to the 5′ end of the H4/Lp4 region. Moreover, the G58 of variant A16G58 was weakly cut by RNase T1 whereas the same residue of variant A16G58.H2 was strongly hit by RNase T1. These results suggest that the stabilization of H2 may induce certain structural rearrangement of HDV ribozyme. The alteration may stimulate the alignment of essential functional groups and stabilize the catalytic core of ribozyme molecule that have positive effect on *cis*-cleavage reaction. Nonetheless, the details of the secondary structure change cannot be resolved by RNase probing.

cis-Cleavage Reaction in the Presence of Formamide. The cleavage rate of the wild type ribozyme Rz 1 decreased as the concentration of formamide increased but the fraction

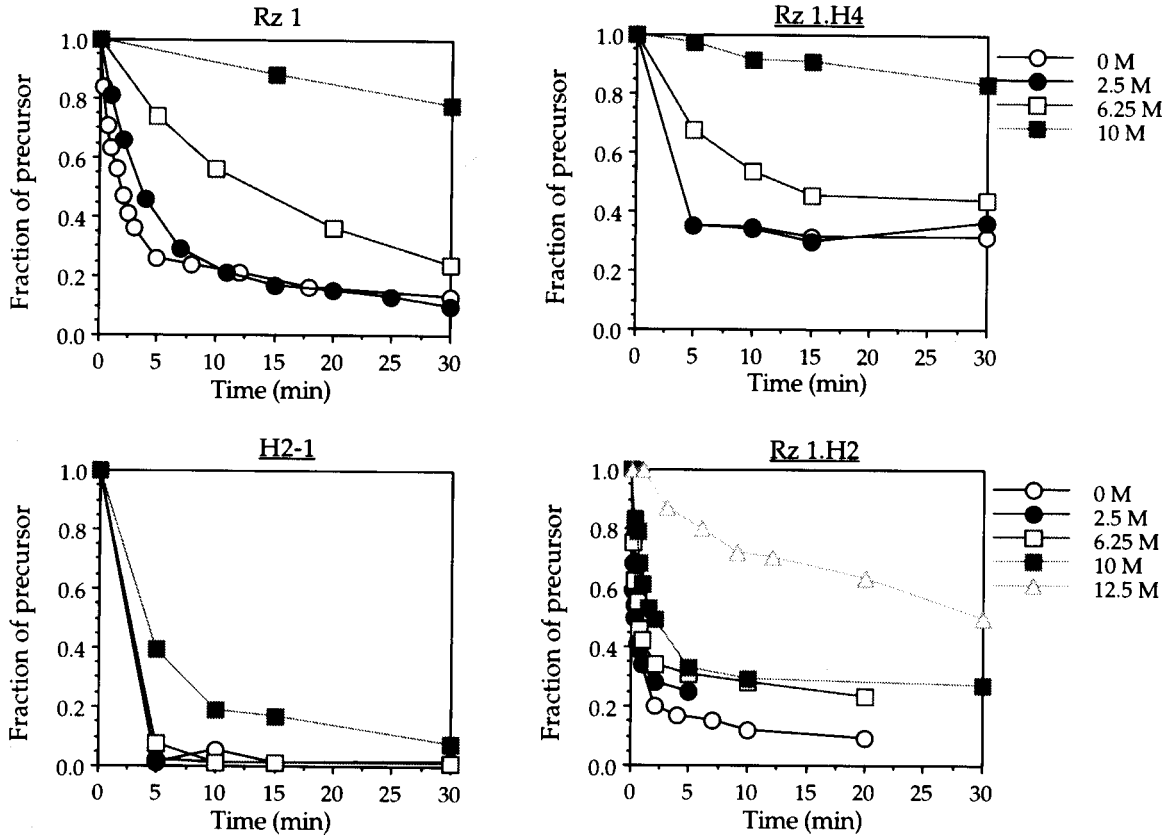

FIGURE 3: Effect of formamide on the *cis*-cleavage reactions of Rz 1 and its H2 or H4 insertion mutants. Variant Rz 1.H4 had five UA base pairs inserted to the top of the H4 of Rz 1, variant H2-1 had five AU base pairs inserted to the base of the H2 of Rz 1, and variant Rz 1.H2 had 5′-C_2A_2-3′ inserted to the A62/A63 of Rz 1.

Table 2: Effect of Formamide on the *cis*-Cleavage Reaction[a]

variant	[formamide] 0 M		2.5 M		6.25 M		10 M		12.5 M	
Rz 1	1.5′	(90%)	4′	(90%)	20′	(90%)	75′	(90%)		(20%)
C16G58	1′	(70%)	1.5′	(70%)	2′	(70%)	5′	(60%)	15′	(45%)
U16U58	1′	(85%)	1′	(70%)	2′	(65%)		(35%)	ND	
C16C58	6′	(80%)	10′	(70%)	13′	(60%)		(30%)	ND	
G16C58	1′	(80%)	1′	(80%)	50′	(60%)		(25%)	ND	
G16U58	1′	(80%)	5.5′	(60%)		(35%)		(25%)	ND	
G16A58	2′	(60%)		(35%)		(20%)	ND		ND	
G16G58	65′	(70%)	60′	(55%)		(35%)	ND		ND	
A16G58	50′	(55%)		(20%)	ND		ND		ND	
Rz 1.H2	0.5′	(90%)	0.2′	(90%)	0.5′	(75%)	1.5′	(80%)	11′	(55%)
C16G58.H2	1.5′	(90%)	1.5′	(90%)	2.5′	(90%)	3′	(90%)	3′	(90%)
C16C58.H2	1′	(90%)	1′	(90%)	3.5′	(90%)	4′	(80%)	16′	(75%)
G16C58.H2	2′	(80%)	3′	(80%)	3.5′	(80%)	5′	(75%)	70′	(70%)
G16G58.H2	2′	(90%)	2′	(90%)	2′	(90%)	5′	(90%)	50′	(80%)
A16G58.H2	5′	(90%)	7′	(90%)	9′	(90%)	30′	(90%)	58′	(75%)

[a] The *cis*-cleavage reaction was conducted in 40 mM Tris-HCl (pH 7.5) and 12 mM $MgCl_2$ at 50 °C in the presence of 0−12.5 M of formamide as described in Materials and Methods. The $t_{1/2}$ values of the *cis*-cleavage reaction as well as the molar ratio of the RNA molecules that undergo *cis*-cleavage are shown. The extent of cleavage after 6 h of incubation is shown if the reaction does not level-off.

of the reactive RNA molecules at the end of *cis*-cleavage reaction, i.e., the extent of cleavage, remained unaltered in the presence of up to 10 M of formamide. The co-incubation with 12.5 M of formamide, however, severely decreased the extent of cleavage (Figure 3, Table 2). Thus, unlike some of the other HDV ribozymes that require denaturant (either formamide or urea) to destabilize the inactive structure(s) of ribozyme molecules and elevate the autolytic activity (Rosenstein & Been, 1990; Wu & Lai, 1990), Rz 1 possesses lower autolytic activity in the presence higher concentrations of formamide. The denaturant may destabilize the catalytic core; consequently, folding into the active structure becomes the rate-limiting step of *cis*-cleavage reaction for Rz 1. We then examined the effect of 0−12.5 M of formamide on the *cis*-cleavage reactions of different ribozyme mutants. The sensitivity to formamide treatment was used to evaluate the stability of the catalytic cores of ribozyme mutants.

The six A16U58 substitution mutants that cleaved at similar rates to that of Rz 1 were studied first (Table 2). Variant C16G58 was very insensitive to formamide. The incubation with 2.5, 6.25, or 10 M of formamide slightly decreased its cleavage rate. In addition, ~50% of the RNA molecules of variant C16G58 were reactive in the presence of 12.5 M of formamide, and they cleaved at a rate only

~15-fold slower than that of in the absence of any denaturant. In the case of variants C16C58 and U16U58, the *cis*-cleavage reactions were barely affected by 2.5 and 6.25 M of formamide, while higher concentrations of formamide significantly decreased their autolytic activities. Both variants G16C58 and G16U58 were quite active in the presence of 2.5 M of formamide. However, the incubation with 6.25 M of formamide severely decreased the rate of *cis*-cleavage or/and the fraction of the reactive RNA molecules. Variant G16A58 cleaved poorly in the presence of 2.5 M of formamide. Therefore, although Rz 1 and these *cis*-cleaving ribozymes possessed similar autolytic activities under the native condition (in the absence of formamide), their resistance to formamide varied with the order of C16G58 > Rz 1 (A16U58) > U16U58 ≃ C16C58 > G16C58 > G16U58 > G16A58. It is notable that there is no direct correlation between the maintenance of Watson−Crick base pairing and the resistance to formamide. The results disclose that the sequence of H2−H3 interface may affect the stability of ribozyme molecule.

Variant Rz 1.H2 that contained a more stable H2 and variant H2-1 that had H2 extended by five AU pairs were more resistant to formamide treatment than that of Rz 1 (Figure 3, Table 1). The insertion of 5′-C_2A_2-3′ to A62/A63's of the A16U58 substitution mutants C16G58, C16C58, G16C58, G16G58, and A16G58 not only enhanced the extent of cleavage but also increased the rate of cleavage in the presence of formamide (Table 2). Likewise, the correlation between the resistance to formamide and the stability of H2 has been observed for a ribozyme derived from HDV antigenomic sense RNA as well (Smith et al., 1992). Nevertheless, the extension of H4 by inserting five UA pairs to the top of H4 did not have such effect (Rz 1.H4, Figure 3). These results disclose that a more stable H2 but not H4 may stabilize the catalytic core and enhance the autolytic activity of HDV ribozyme.

The trans-Cleaving Ribozyme

We have constructed a bimolecular construct RNA73/RNA37 by dividing a *cis*-cleaving HDV ribozyme into two subdomains from regions $J_{1/2}$ and Lp4 after the wild type 5′ and 3′ termini were ligated (Lai et al., 1996). The ribozyme subdomain (RNA37) may interact with the substrate subdomain (RNA73) that contains circularly permuted sequences through the formation of H1, H2, and H4 to reconstitute the pseudoknot-like structure of HDV autolytic domain (Figure 4). In addition, the ribozyme catalyzed the site-specific cleavage of the substrate *in trans* (Lai et al., 1996). In this study, we elongated the H2 of construct RNA73/RNA37 from 5 to 10 base pairs long by inserting 5′-GCU-3′ to near the 5′ terminus of the ribozyme molecule. The new construct was named RNA73/LH2RNA37 (Figure 4). The effects of H2 extension on the *trans*-cleavage reaction of HDV ribozyme was investigated.

Single-Turnover Reaction. The *trans*-cleavage of RNA73 was followed under single-turnover conditions with ribozyme in excess of substrate. The cleavage of RNA73 was not completed even though it was incubated with 50 molar excess of ribozyme, and the extent of cleavage leveled off at 50% and 60% for constructs RNA73/RNA37 and RNA73/LH2RNA37, respectively (data not shown). For both bimolecular constructs, there was an initial lag of product

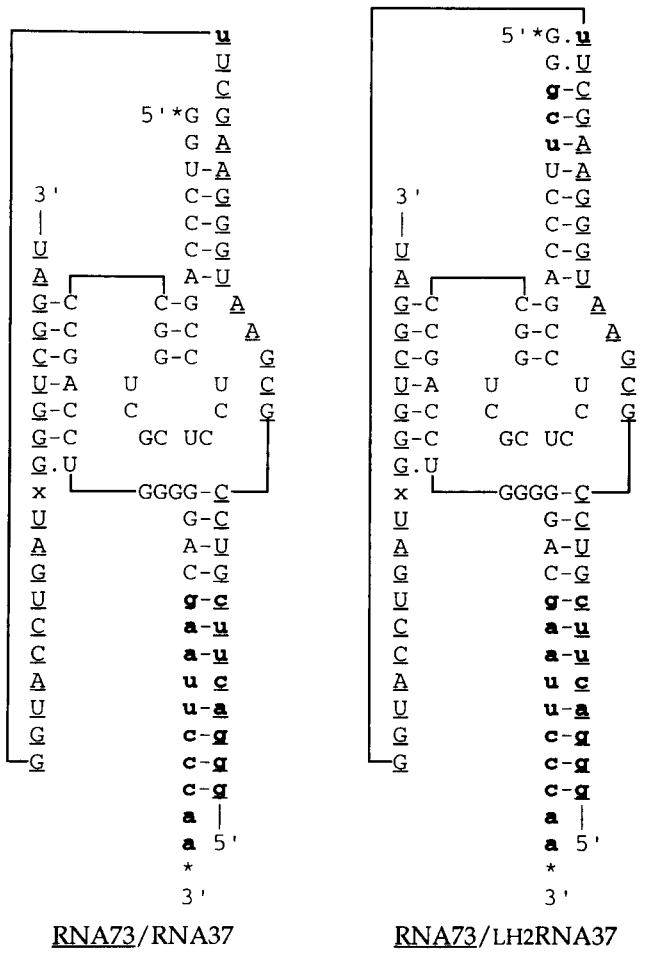

FIGURE 4: Sequence and proposed secondary structure of the bimolecular constructs RNA73/RNA37 and RNA73/LH2RNA37. The reconstitution of the pseudoknot-like structure of HDV autolytic domain relies on the base-pairing interactions of H1, H2, and H4. Residues of the substrate subdomain (RNA73) are underlined. Residues of the substrate and ribozyme subdomains that are different from those of Rz 1 are illustrated by lower case bold letters.

formation if the substrate and ribozyme RNA's were not pre-annealed. The co-denaturation and renaturation treatment of substrate and ribozyme RNA's enhanced the rate of product formation (Figure 5A and B). In addition, the cleavage reactions of both constructs followed the first order kinetics if two subdomains were pre-annealed. Thus, the pre-annealing of two subdomains may facilitate the assembly and/or the conformational rearrangement of substrate/ribozyme complex for catalysis.

Experiments with pre-annealed substrate and ribozyme RNA's were then used to estimate the cleavage rate constants of constructs RNA73/RNA37 and RNA73/LH2RNA37. The rate of product formation was measured in the reactions with ribozyme in excess of substrate, therefore, a complete *trans*-cleavage reaction did not require product release. The single-turnover rate (k_{ob}) increased with increasing concentrations of ribozyme, and the cleavage rate approached a constant value at ribozyme concentrations above 50 nM (Figure 5C). The cleavage rate constant (k_2) and K'_M, respectively, were derived from the *Y*-intercept and the slope of the plot of k_{ob} versus k_{ob}/[R] (Figure 5D). The k_2 of construct RNA73/LH2RNA37 was ~6-fold higher than that of construct RNA73/RNA37 (0.98 min^{-1} versus 0.17 min^{-1}), while there was only a 2-fold difference between the K'_M of two constructs (~30 nM for the former and ~15 nM for the later).

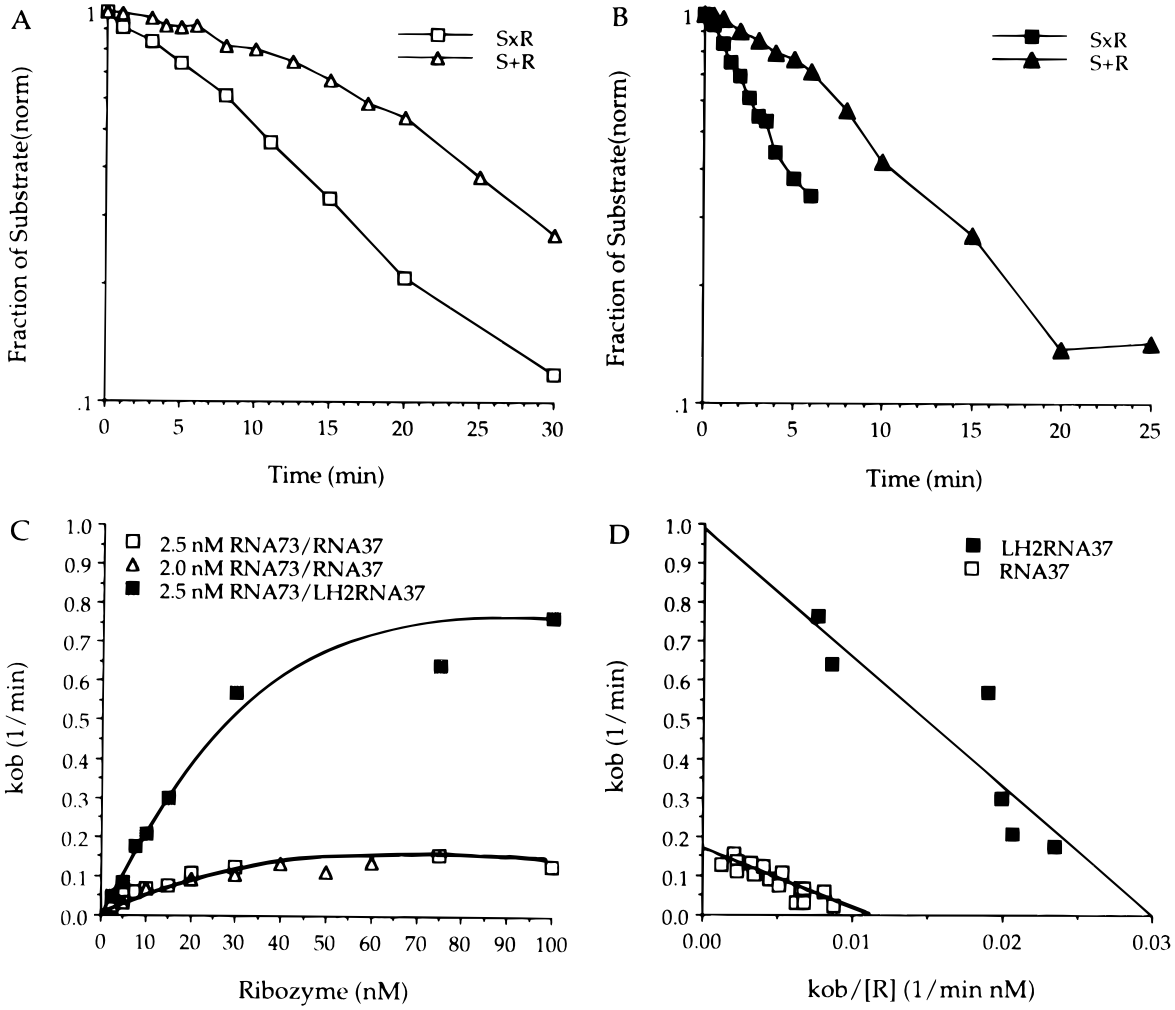

FIGURE 5: Single-turnover reactions of constructs RNA73/RNA37 and RNA73/LH2RNA37. (A, B) The pre-annealing of substrate and ribozyme RNA's promotes single-turnover reactions. 2.5 nM of substrate (RNA73) and 10 nM of ribozyme [RNA37 for A and LH2RNA37 for B] were pre-annealed (S×R) or not (S+R) before the initiation of *trans*-cleavage reaction. The amount of substrate remaining was normalized to the reactive species of each bimolecular construct. The rate constant (k_{ob}) was derived from the first-order disappearance of reactive substrate. With pre-annealed RNA's, the value of k_{ob} was 0.07 min^{-1} for construct RNA73/RNA37 and 0.24 min^{-1} for construct RNA73/LH2RNA37. (C, D) The elongation of H2 stimulates single-turnover reaction. The substrate and ribozyme RNA's have been pre-annealed. Rates constants for reactions with fixed amount of substrate and varying concentrations of ribozyme were obtained from the first-order disappearance of reactive substrate. The plots of k_{ob} versus ribozyme concentration, [R], are shown in C. The plots of k_{ob} versus k_{ob}/[R] are shown in D.

The results illustrate that the elongation of H2 elevates the *trans*-cleavage rate.

Furthermore, the *trans*-cleavage reactions were carried out in the presence of 0−10 M of formamide (Table 3). The cleavage rate of construct RNA73/RNA37 decreased as the concentration of formamide increased; in addition, the *trans*-cleavage reaction did not occur in the presence of 10 M of formamide. Construct RNA73/LH2RNA37 was more resistant to denaturant treatment. The concentration of formamide could be as high as 7.5 M without significantly affecting the cleavage rate (k_{ob}) and the co-incubation with 10 M of formamide decreased the cleavage rate ~10-fold. Thus, similar to that of the *cis*-cleaving HDV ribozymes, the elongation of the H2 of the bimolecular construct enhances the resistance to formamide as well. It is notable that the co-incubation with formamide slightly increased the amount of the reactive species of substrate molecules for both bimolecular constructs (Table 3). It is likely that optimum amount of denaturant may elevate the extent of cleavage by destabilizing certain alternative substrate/ribozyme complex(es) and substrate/substrate complex(es).

Table 3: Effect of Formamide on the *trans*-Cleavage Reactions of Constructs RNA73/RNA37 and RNA73/LH2RNA37[a]

	ribozyme RNA37		ribozyme LH2RNA37	
[formamide]	k_{ob} (min^{-1})	S_{active}	k_{ob} (min^{-1})	S_{active}
0 M	0.070	50%	0.24	60%
1.25 M	0.050	50%	0.20	60%
2.5 M	0.047	60%	0.18	60%
5 M	0.027	70%	0.35	70%
7.5 M		30% (3 h)	0.17	70%
10 M		0% (3 h)	0.02	55%

[a] The cleavage of 2.5 nM of RNA73 catalyzed by 10 nM of RNA37 or LH2RNA37 in 40 mM Tris-HCl (pH 7.5) and 12 mM $MgCl_2$ at 50 °C. The substrate and ribozyme RNA's were co-denatured and renatured in the presence of 0−10 M of formamide before the initiation of *trans*-cleavage. The k_{ob}'s are the rates of the first-order disappearance of reactive substrate RNA73. S_{active} is the fraction of RNA73 that has been cleaved, and the value after 3 h of incubation is shown if the *trans*-cleavage does not level-off.

Multiple-Turnover Reaction. In the multiple-turnover reaction catalyzed by 2.5 nM of RNA37, each ribozyme molecule on an average catalyzed the cleavage of eight molecules of RNA73, and almost all of the cleavable RNA73

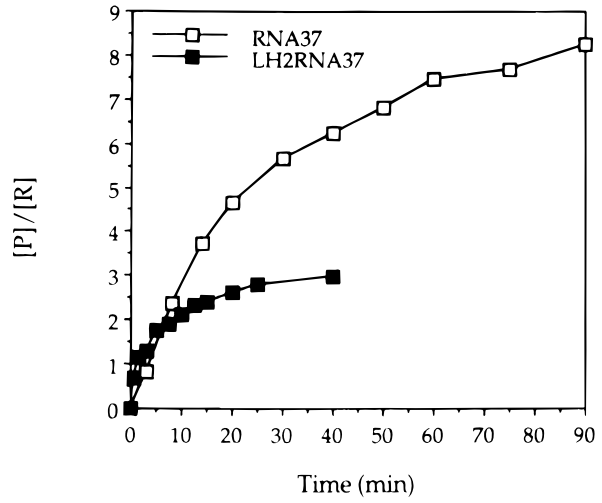

FIGURE 6: Effect of the elongation of H2 on multiple-turnover reactions. 40 nM of substrate (RNA73) was pre-annealed with 2.5 nM of ribozyme before the initiation of *trans*-cleavage reaction. The number of moles of product generated per mole of ribozyme ([P]/[R]) versus reaction time is plotted. The *trans*-cleavage reaction was catalyzed by RNA37 or LH2RNA37.

molecules were digested after 100 min of incubation (Figure 6). However, the cleavage rate became slower at later times; therefore, product release may occur at a rate slower than or on the same order as the cleavage process for this bimolecular construct. Nevertheless, there was an initial burst of product formation followed by slower product formation for the cleavage of RNA73 catalyzed by 2.5 nM of LH2RNA37. In addition, the maximum turnover number did not exceed 3 (Figure 6). The elongation of H2 may significantly enhance the affinity between the 5′-cleavage product and ribozyme molecule. This speculation is consistent with the finding that when the 5′-cleavage product of RNA73 was incubated with excess amount of ribozyme, ribozyme LH2RNA37 formed cleavage product/ribozyme complex that persisted through native gel electrophoresis at lower concentrations than that of ribozyme RNA37 (data not shown). Thus, product release is rate limiting for construct RNA73/LH2RNA37, and the subsequent binding of intact substrate is hindered.

SUMMARY

The HDV *cis*-cleaving ribozyme derived from the autocatalytic domains of HDV genomic and antigenomic senses RNA contains four helical regions (H1, H2, H3, and H4). Two of the helices (H2 and H3) may stack coaxially. Hence, the ribozyme molecule is likely to adopt a pseudoknot-like structure (Perrotta & Been, 1991). In this study we have shown that the H2 of HDV ribozyme could be extended to twice of its original size without affecting *cis*-cleavage reaction. Nevertheless, the deletion or substitution mutations that destabilized H2 and the introduction of a bulged residue to the junction of H2 and H3 greatly decreased autolytic activity. Therefore, the helical structure of H2 as well as the continuity of H2 and H3 are important for the folding of ribozyme molecule, but H2 by itself may protrude away from the catalytic center as proposed in the 3D structural model (Tanner et al., 1994).

The A16U58 of ribozyme Rz 1 was substituted to all possible sequences to investigate the effect of H2-H3 interface sequence on the autolytic activity of HDV ribozyme. The mutational analysis discloses that AG, AA, AC, and GG mismatched base pairs were the least favorable sequences of nucleotides 16 and 58 of Rz 1 since the corresponding mutants *cis*-cleaved at significantly lower rates than ribozyme Rz 1 whereas all of the other A16U58 substitution mutants *cis*-cleaved reasonably well. Thus, the sequence of the last base pair of H2 rather than its base-pairing interaction affects the catalytic core. Moreover, the stability of the catalytic cores of certain A16U58 substitution mutants were compared by detecting the effect of formamide on their *cis*-cleavage reactions. The results reveal that the stability of the catalytic core of ribozyme molecule is affected by H2−H3 interface sequence. Nevertheless, there was no direct correlation between the maintenance of the helical structure of H2 and the stability of the catalytic core since variants U16U58 and C16C58 possessed higher autolytic activities than variants G16C58 and G16U58 in the presence of 6.25 M of formamide. In addition, for certain A16U58 substitution mutants, the resistance to the denaturant treatment did not follow the order of the sequence dependence of stability of the coaxially stacked interfaces (Walter & Turner, 1994). For instance, the resistance to formamide has the order of variant C16G58 > Rz 1 (A16U58) > variant G16C58, while the thermodynamic parameter of coaxial stacking helices has the order of 5′GC (represents the last base pair of H2)-5′GC (represents the first base pair of H3) > 5′CG-5′GC > 5′AU-5′GC. Thus, the steric constrains associated with the direct linkage of H1, H2, and H3 may distort the coaxial helices of H2 and H3 and disrupt the base-pairing interaction between nucleotides 16 and 58.

H2 and H4 are essential structural elements of HDV ribozyme. Nevertheless, unlike that of the other two double-stranded regions, H2 and H4 can be variable in size and in sequence (Wu & Huang, 1992; Wu et al., 1993). These two helices may extend out of the catalytic center of ribozyme molecule. In this study we have found that the extension of the H2 region may facilitate the *cis*-cleavage reaction of HDV ribozymes by elevating the cleavage rate and enhancing the stability of the catalytic core. However, the elongation of the H4 region of HDV ribozyme does not have such effects. In addition, an extended H2 may compensate for the negative effects on the *cis*-cleavage reaction/the folding of HDV ribozyme that include the disturbance of the continuity of H2 and H3, the unfavorable sequences at the bottom of H2, as well as the mismatched base pair(s) in H2. We propose that a more stable H2 not only facilitates guide the folding of the catalytic core but also alters the rate limiting step of *cis*-cleavage reaction. Moreover, the ribonuclease probing experiment has illustrated that an extended H2 may alter the conformation of HDV ribozyme. The extended H2 is likely to participate in tertiary interactions that alter the structure of ribozyme molecule, and the structural alteration may stimulate the alignment of the functional groups that are involved in catalysis.

Furthermore, the elongation of H2 may stimulate the reconstitution of the pseudoknot-like structure of the *trans*-cleaving HDV ribozyme (RNA73) and its substrate (RNA37) that rely on the base-pairing interactions of H1, H2, and H4. The stronger base-pairing interaction of the extended H2 in the bimolecular construct stabilizes the catalytic core and elevates the *trans*-cleavage rate, whereas the release of cleavage product from the ribozyme RNA is inhibited. A more stable H2 also has a positive effect on the *trans*-

cleavage reaction of HDV ribozyme. However, unlike that of the hammerhead ribozymes (Dahm et al., 1993), the *cis*- and the *trans*-cleavage reactions of HDV ribozymes are insensitive to pH change between pH 6.5 and 8 [Wu et al. (1989) and unpublished observations of this laboratory]. Therefore, it is hard to distinguish whether the effect of the elongation of the H2 region is due to the stimulation of the chemical process of cleavage reaction or the enhancement of the rate of conformation rearrangements.

REFERENCES

Dahm, S. S., Derrick, W. B., & Uhlenbeck, O. C. (1993) *Biochemistry 32*, 13040−13045.

Hampel, A., Tritz, R., Hicks, M., & Crutz, P. (1990) *Nucleic Acids Res. 18*, 299−304.

Kawakami, J., Kummar, P. K. R., Suh, Y. A., Nishikawa, F., Kawakami, K., Taira, K., Ohtsuka, E., & Nishikawa, S. (1993) *Eur. J. Biochem. 217*, 29−36.

Kos, A., Dijkema, R., Amberg, A. C., van der Meidie, P. H., & Schelleken, H. (1986) *Nature (London) 323*, 558−560.

Kummar, P. K. R., Suh, Y. A., Miyashiro, H., Nishikawa, F., Kawakami, J., Taira, K., & Nishikawa, S. (1992) *Nucleic Acids Res. 20*, 3919−3924.

Kuo, M. Y.-P., Sharmeen, L., Dinter-Gottlieb., & Taylor, J. (1988) *J. Virol. 62*, 4439−4444.

Lai, Y. C., Lee, J. Y., Liu, H. J., Lin, J. Y., & Wu, H. N. (1996) *Biochemistry 35*, 124−131.

Macnaughton, T. B., Wang, Y. J., & Lai, M. M. C. (1993) *J. Virol. 67*, 2228−2234.

Makino, S., Chang, M. F., Shieh, C. K., Kamahora, T., Vannier, D. M., Govindarajan, S., & Lai, M. M. C. (1987) *Nature (London) 329*, 343−346.

Perrotta, A. T., & Been, M. (1990) *Nucleic Acids Res. 18*, 6821−6827.

Perrotta, A. T., & Been, M. (1991) *Nature (London) 350*, 434−436.

Rosenstein, S. P., & Been, M. (1990) *Biochemistry 29*, 8011−8016.

Rosenstein, S. P., & Been, M. (1991) *Nucleic Acids Res. 19*, 5409−5416.

Sanger, F., Nicklen, S., & Coulson, A. R. (1977) *Proc. Natl. Acad. Sci. U.S.A. 74*, 1074−1078.

Smith, J. B., Gottlieb, P. A., & Dinter-Gottlieb, G. (1992) *Biochemistry 31*, 9629−9635.

Suh, Y. A., Kumar, P. K. R., Taira, K., & Nishikawa, S. (1993) *Nucleic Acids Res. 21*, 3277−3280.

Tanner, N. K., Schaff, S., Thill, G., Petit-Koskas, E., Crain-Denoyelle, A.-M., & Westhof, E. (1994) *Curr. Biol. 4*, 488−498.

Thill, G., Vasseur, M., & Tanner, N. K. (1993) *Biochemistry 32*, 4254−4262.

Uhlenbeck, O. C. (1987) *Nature (London) 350*, 434−436.

Walter, A. E., & Turner, D. H. (1994) *Biochemistry 33*, 12715−12719.

Wang, K. S., Choo, Q. L., Weiner, A. J., Ou, J. H., Najarian, R. A., Thayer, R. M., Mullenbach, G. T., Denniston, K. L., Gerin, J. L., & Houghton, M. (1986) *Nature (London) 323*, 508−515.

Wu, H. N., & Lai, M. M. C. (1990) *Mol. Cell. Biol. 10*, 5575−5579.

Wu, H. N., & Huang, Z. S. (1992) *Nucleic Acids Res. 20*, 5937−5941.

Wu, H. N., Lin, Y. J., Lin, F. P., Makino, S., Chang, M. F., & Lai, M. M. C. (1989) *Proc. Natl. Acad. Sci. U.S.A. 86*, 1831−1835.

Wu, H. N., Wang, Y. J., Hung, C. F., Lee, H. J., & Lai, M. M. C. (1992) *J. Mol. Biol. 223*, 233−245.

Wu, H. N., Lee, J. Y., Huang, H. W., Huang, Y. S., & Hsueh, T. G. (1993) *Nucleic Acids Res. 21*, 4193−4199.

BI961219M